Electrodeposition of Fe—Pt Films with Low Oxide Content Using an Alkaline Complexing Electrolyte

Defu Liang, Jonathan J. Mallett,† and Giovanni Zangari*

Department of Materials Science and Engineering and CESE, University of Virginia, Charlottesville, Virginia 22904-4745

ABSTRACT Electrochemical deposition of equiatomic Fe—Pt from complexing electrolytes provides precise tuning of alloy stoichiometry, enables close control of the growth process, and results in limited oxygen incorporation. The films grow epitaxially on oriented substrates and the low oxygen content favors transformation from the as-deposited cubic to the high anisotropy $L1_0$ phase and magnetic hardening upon thermal annealing at temperatures (400—450 °C) much lower than previously achieved by other plating processes.

KEYWORDS: electrodeposition • underpotential • Fe—Pt • magnetic films • hard magnetic materials • magnetic recording

INTRODUCTION

The $L1_0$ superlattice phase of equiatomic Fe—Pt is a highly promising material for magnetic data storage devices because of its large magnetocrystalline anisotropy energy (1). This property would allow the magnetic nanofeatures envisioned for future patterned hard disk media or spin torque transfer (STT) MRAM devices to be stable against spontaneous magnetization reversal and consequent data loss. The desired $L1_0$ superlattice structure is the equilibrium phase of Fe—Pt below 1300 °C, but materials deposited at temperatures below about 400 °C lack the required degree of long-range order (2) because of the limited mobility of atomic species during deposition. High-temperature annealing of up to 650 °C is required to form the equilibrium phase (3), but this is incompatible with most polymer-based lithography methods and would likely result in interdiffusion between different layers of a device structure. Chemical synthesis and subsequent self-assembly of nanoparticles (4–6) has also been extensively explored for media applications but still requires high-temperature annealing to achieve the desired chemical order, which invariably results in sintering of the particles. A low-temperature deposition method is needed that can maximize the degree of as-deposited local order, thereby reducing the severity of any post deposition annealing needed to achieve complete order. Electrodeposition has the advantage over most deposition methods of allowing material to be deposited close to the equilibrium condition between atoms in the solid phase and ions in solution. Under the appropriate conditions, this can be used to thermodynamically control the composition and in some cases the crystal structure of the deposit. An additional advantage of electrodeposition is its ability to uniformly fill high aspect ratio template features, with none of the shadowing problems associated with line-of-sight vacuum deposition techniques.

However, electrochemical codeposition of Fe with Pt is challenging. At the very negative potentials required to deposit Fe, hydrogen gas evolution also occurs and, furthermore, this parasitic reaction is strongly catalyzed at a Pt (alloy) surface. This can cause local pH shifts that result in iron hydroxide/oxide incorporation into the deposits. The negative deposition potential is also problematic for platinum deposition from weakly complexing solutions. Under these conditions, the driving force for Pt reduction reaction is large, such that the Pt deposition rate becomes limited by the diffusion of the Pt complex to the growth interface. This type of diffusion limited growth is well-known to result in growth instabilities (7), leading to porous films.

An electrodeposition process has been reported (8, 9) that attempted to mitigate the issues described above by depositing Fe—Pt at more positive potentials than would be energetically possible for pure Fe deposition. This is due to the strongly exothermic mixing of Fe and Pt in the alloy and was described at equilibrium in terms of a regular solution model of alloying (8). Unfortunately, in the case of Fe—Pt the positive shift in deposition potential was insufficient to prevent the incorporation of up to 30 at % oxygen into the equiatomic alloy (8, 9). High-temperature annealing in reducing atmosphere was therefore necessary to fully develop the hard magnetic properties of the ordered phase.

In the present study, a growth process that deals with both the issues of the morphological stability of Pt deposition and of hydroxide/oxide incorporation is reported. Morphological stability of Pt deposition is readily achieved by replacing the weakly complexed Pt(IV) in chloroplatinic acid previously used for Fe—Pt electrodeposition with the much stronger amino-nitrite Pt(II) complex. This stronger complexation allows Pt to be deposited at a rate controlled by the kinetics of electrochemical reduction, even at the nega-

* Corresponding author. E-mail: gz3e@virginia.edu.
Received for review January 22, 2010 and accepted March 11, 2010
† Current address: American Physical Society, 1 Research Road, Ridge, New York.
DOI: 10.1021/am100066x

tive potentials required for Fe codeposition, and leads to compact, smooth deposits. The viability of this complex for pure Pt electrodeposition is now well-established (10), but its stability is restricted to solutions of pH ranging from 8−10. This presents further challenges with respect to iron hydroxide precipitation, necessitating strong iron complexation. We show that a combination of citrate and glycine provides sufficient complexation and pH buffering to drastically reduce hydroxide precipitation (citrate alone has been found to be insufficient in this respect (11)). A similar combination of additives has also been used to successfully deposit Co-rich Co−Pt alloys (12, 13). Deposition of Fe−Pt films from a similar electrolyte, adjusted at pH 2.5, was recently reported (14). However, at the chosen pH and concentration of complexing agents, the measured oxygen content was above 20 at %.

EXPERIMENTAL METHODS

The electrolyte used for Fe−Pt electrodeposition contained $Fe_2(SO_4)_3$ 50 mM, $Pt(NH_3)_2(NO_2)_2$ 15 mM, $(NH_4)_2SO_4$ 0.1 M, $NaNO_2$ 0.1 M, NH_2CH_2COOH 0.15 M, $(NH_4)_2C_6H_6O_7$ 0.15 M (15). All solutions were adjusted to pH 8 by the addition of potassium hydroxide. Deposition was performed under quiescent conditions at 75 °C, in a cylindrical cell that was heated using a water jacket. A Pt-grid counter electrode was used, along with a saturated sulfate electrode (SSE). The latter was separated from the main cell using a salt bridge, allowing it to be operated close to room temperature. Deposition potentials are reported with respect to a calomel reference electrode (SCE) to facilitate comparison to previous work (8, 9). All electrochemical experiments were performed in a three-electrode cell using an EG&G Princeton Applied Research potentiostat-galvanostat model 283. Fe−Pt films were electrodeposited at constant applied potential onto 100 nm thick Ru or Cu seed layers that had been sputter deposited onto the native oxide of Si(100). Cu(200) substrates were obtained by sputtering Cu onto hydrogen-terminated Si(100) wafers.

Crystal structure was investigated by X-ray diffraction (XRD), using a Scintag XDS 2000 diffractometer with Cu K_α radiation ($\lambda = 1.5406$ Å) in the $\theta/2\theta$ geometry. Alloy composition was determined by an energy-dispersive spectroscopy (EDS) detector attached to a JEOL JSM-6700F scanning electron microscope. The oxygen content was measured by Auger electron spectroscopy (AES, Perkin-Elmer PHI 660 Scanning Auger Multiprobe). Hysteresis loops were collected using a vibrating sample magnetometer (VSM, Lakeshore 7400), both in the plane and perpendicular geometry, up to 2 T (20 kOe).

RESULTS AND DISCUSSION

Iron is added to the solution in the form of Fe(III) sulfate, which is its highest oxidation state. In this way there is no chance of the iron ions in solution to be further oxidized by residual dissolved oxygen. The combination of citrate and glycine added to the solution reduces the concentration of free Fe^{3+} ions to below the precipitation threshold for iron(III) hydroxide and provides for solution stability over time. The electrodeposition of Fe is thought to occur in a two-step reduction process; Fe(III) species are reduced to Fe(II) in the first step and subsequently further reduced to Fe metal in the second reaction step. Electrochemical data indicate that the first step proceeds at a rate that is limited by transport of Fe(III) to the electrode from the solution bulk. Under these conditions, the Fe(III) concentration near the electrode surface is depleted by the reaction to almost zero and the total concentration of Fe(II) species generated near the electrode is approximately the same as the bulk concentration of Fe(III). Citrate and glycine are also known to complex Fe^{2+} strongly, reducing the concentration of free Fe^{2+} near the electrode to well below the total Fe(II) concentration. This has the benefit of preventing Fe(II)hydroxide precipitation. The second reaction step is thought to occur close to equilibrium between the Fe(II) species in the solution near the electrode and Fe metal in the alloy deposit.

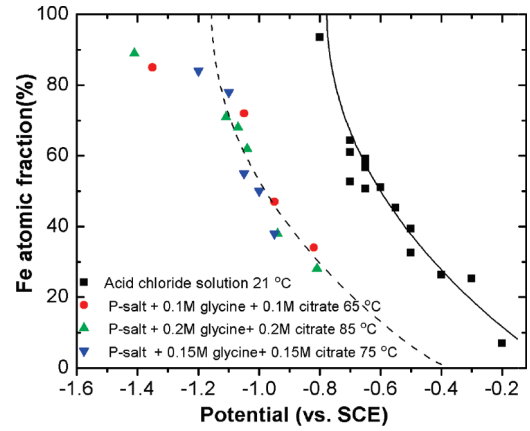

FIGURE 1. Dependence of Fe−Pt film composition on deposition potential for films deposited from chloride solutions (squares) and from amino-nitrite/citrate/glycine solutions (circles and triangles). The solid curve is a subregular solution model fit to the square data points. The dashed curve was obtained by shifting the solid curve to fit the other data sets.

Figure 1 shows the dependence of film composition as determined by EDS on the applied potential for films deposited from the strongly complexing solution (circles and triangles). These data are compared with published data, obtained from simple chloride solutions (squares) (8). The offset of these two data sets is attributed to the shift in the equilibrium potential of pure Fe resulting from the combined strength of the citrate (16) and glycine (17) complexation. This drastically reduces the free Fe^{2+} activity causing a negative shift in the equilibrium potential for Fe deposition. The observed potential dependence of the alloy composition can be explained using a thermodynamic model that incorporates the heat of mixing in the alloy deposit, as described previously (8). A fit to this model was used to produce the solid curve, taken from ref 8. The dashed curve is the same as the solid curve, only shifted in potential by 350 mV to take into account the thermodynamic effect of Fe^{2+} complexation by citrate and glycine. Because these curves assume that Fe deposition occurs close to equilibrium, the close fit with experiments suggests that the conditions of Fe^0/Fe^{2+} equilibrium are closely followed under the chosen experimental conditions, except for the Fe-rich films, where kinetic overpotentials become important. Conditions approximating an interfacial equilibrium were achieved by depositing the alloy slowly (between 50−250 nm/h), through the use of a low Pt concentration. The predictable dependence of composition on applied potential is useful for ensuring reliable control of stoichiometry. In particular,

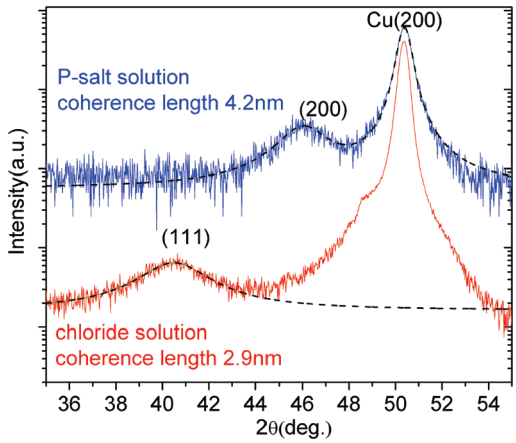

FIGURE 2. XRD data for 100 nm near equiatomic Fe—Pt films deposited onto Cu (200) from chloride and amino-nitrite/citrate/glycine solutions.

equiatomic Fe—Pt films were grown at 75 °C, −1.03 V_{SCE}, at a rate of 100 nm/h.

The combined effects of strong iron complexation and buffering reduced the atomic fraction of oxygen in equiatomic Fe—Pt films to about 2—4 at % (as estimated by EDS) or about 6 at % (as determined by AES), compared with up to 30 at % for films deposited from chloride solutions (8, 9). The oxide content did not show any dependence on composition. This reduction in oxide content has significant implications for the magnetic properties of the films. Levels of oxide in excess of 10 % have been found to persist in films prepared by previous methods, even after annealing in pure hydrogen for extended periods at 600 °C (18).

Depositing Pt from the stronger amino-nitrite complex also has beneficial effects on the growth control of as-deposited films. Figure 2 shows XRD data for 100 nm thick films of near-equiatomic Fe—Pt deposited onto Cu (200) substrates from the amino-nitrite/citrate/glycine solution and from a simple chloride solution. The as-deposited films exhibit a face-centered cubic FCC structure. The most obvious difference is the strong (200) texture in the case of the former compared with the (111) texture of the latter. It is also notable that the coherence length obtained for the chloride solution using the Scherrer equation was 2.9 nm compared with 4.2 nm for the amino-nitrite/citrate/glycine solution. This (200) texture is useful for device applications that require perpendicular anisotropy, but has not before been realized in as-deposited electroplated films.

Figure 3 shows the effect upon the crystal structure and magnetic properties of annealing 100 nm thick near-equiatomic Fe—Pt films deposited onto unoriented Ru substrates from the amino-nitrite/citrate/glycine solution. (These substrates were chosen for the annealing study rather than the Cu (100) to avoid known issues of silicide formation by interdiffusion of the film and substrate.) The annealing was performed in forming gas (5 % H_2 and 95 % Ar), for 60 min, first at 400 °C and then at 450 °C. Magnetic hardening is observed to occur in correspondence with phase transformation from the as-deposited FCC to the equilibrium $L1_0$ phase at 400 °C, as detected by the splitting of the (200) and (002) peaks and by the presence of the superlattice (001)

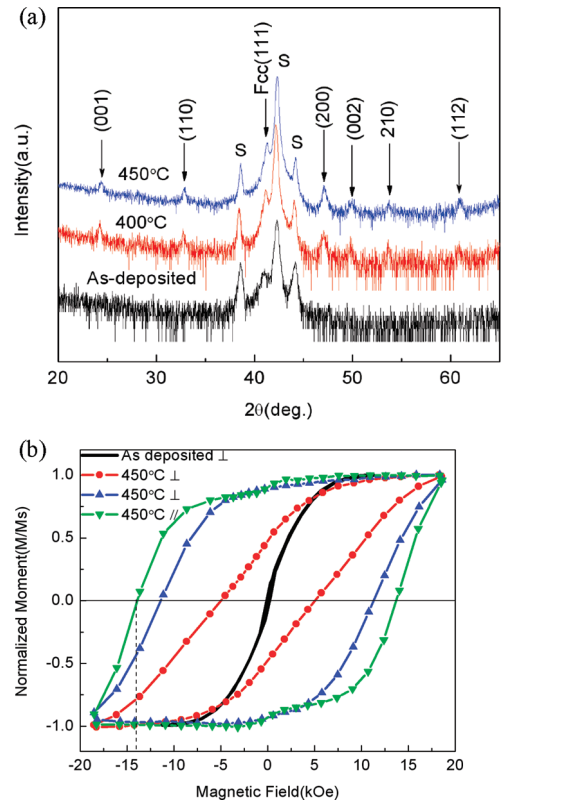

FIGURE 3. (a) XRD data and (b) magnetic hysteresis curves for as-deposited and annealed near-equiatomic Fe—Pt films, 100 nm thick.

peak, and to fully develop already at 450 °C. The coercivity of 13.8 kOe is to our knowledge the highest reported for any electrodeposited material, and the measured magnetic moment of about 1.1 T (77 % of the bulk value, slightly decreased upon annealing) suggests low porosity and limited incorporation of nonmagnetic matter. This annealing temperature is about 200 °C lower than was required to achieve similar coercivities in films produced by other plating methods. This is very promising from the point of view of device fabrication, because it may minimize damage to template structures, seed layers, or microstructure.

CONCLUSION

Fe—Pt films were electrodeposited from a complexing amino-nitrite/citrate/glycine electrolyte under kinetic control for Pt reduction and near equilibrium conditions for Fe reduction, ensuring reliable control of alloy composition and limiting oxygen content in equiatomic films to 5—7 at %. The slow deposition kinetics favors epitaxial growth of Fe—Pt films onto oriented templates, and the low oxygen content facilitates phase transformation and magnetic hardening upon thermal annealing at 400—450 °C in forming gas. The combination of near-room-temperature deposition, fine composition control, reduced oxide content, texture control, and reduced annealing temperature for ordering, recommends the present technique for magnetic device applications.

Acknowledgment. Financial support through Grant NSF DMR 0705042 is gratefully acknowledged. Auger Electron Spectroscopy measurements were performed at MAIC, University of Florida.

Supporting Information Available: Electrochemical and electrochemical quartz crystal microbalance data for Pt and Fe deposition, and atomic force microscopy images for equiatomic Fe—Pt films deposited from acidic chloride and amino-nitrite/citrate/glycine electrolytes. This material is available free of charge via the Internet at http://pubs.acs.org.

REFERENCES AND NOTES

(1) Weller, D.; Moser, A.; Best, M. E.; Lee, W.; Toney, M. F.; Schwickert, M.; Thiele, J. U.; Doerner, M. F. *IEEE Trans. Magn.* **2000**, *36*, 10.

(2) Toney, M. F.; Lee, W.-Y.; Hedstrom, J. A.; Kellock, A. *J. Appl. Phys.* **2003**, *93*, 9902.

(3) Ouchi, K. *IEEE Trans. Magn.* **2001**, *37*, 1217.

(4) Sun, S.; Murray, C. B.; Weller, D.; Folks, L.; Moser, A. *Science* **2000**, *28*, 1989.

(5) Sun, S. *Adv. Mater.* **2006**, *18*, 393.

(6) Wellons, M. S.; Morris, III, W. H.; Gai, Z.; Shen, J.; Bentley, J.; Wittig, J. E.; Lukehart, C. M. *Chem. Mater.* **2007**, *19*, 2483.

(7) Aogaki, R.; Kitazawa, K.; Kose, Y.; Fueki, K. *Electrochim. Acta* **1980**, *25*, 965.

(8) Mallett, J. J.; Svedberg, E. B.; Sayan, S.; Shapiro, A. J.; Wielunski, L.; Madey, T. E.; Egelhoff, W. F., Jr.; Moffat, T. P. *Electrochem. Solid-State Lett.* **2004**, *7*, C121.

(9) Leistner, K.; Backen, E.; Schupp, B.; Weisheit, M.; Schultz, L.; Schlorb, H.; Fahler, S. *J. Appl. Phys.* **2004**, *95*, 7267.

(10) Rao, Chepuri, R. K.; Trivedi, D. C. *Coord. Chem. Rev.* **2005**, *249*, 613.

(11) Leistner, K.; Schaaf, p.; Voss, A.; Fähler, S.; Schultz, L.; Schlorb, H. *Electrochim. Acta* **2008**, *53*, 6973.

(12) Pattanaik, G.; Zangari, G.; Weston, J. *Appl. Phys. Lett.* **2006**, *89*, 112506.

(13) Pattanaik, G.; Kirkwood, D. M.; Xu, X.; Zangari, G. *Electrochim. Acta* **2007**, *52*, 2755.

(14) Cherevko, S.; Fu, J.; Song, K. Y.; Chung, C.-H. *Korean J. Chem. Eng.* **2009**, *26*, 1766.

(15) The Pt amino-nitrite complex was synthesized from H_2PtCl_6 (Fischer), via dropwise addition of an excess of $NaNO_2$ to a H_2PtCl_6 solution heated at 100°C, followed by addition of diluted NH_3 to the resulting solution at room temperature. The flocculated precipitate was filtered, washed and used.

(16) Konigberger, L.; Konigberger, E.; May, P. M.; Hefter, G. T. *J. Inorg. Biochem.* **2000**, *78*, 175.

(17) Kiss, T.; Sovago, I.; Gergely, A. *Pure Appl. Chem.* **1991**, *63*, 597.

(18) Leistner, K.; Thomas, J.; Schlorb, H.; Weisheit, M.; Schultz, L.; Fahler, S. *Appl. Phys. Lett.* **2004**, *85*, 3498.

AM100066X